Optical fiber properties of individual human cones

Austin Roorda

University of Houston College of Optometry, Houston, TX, USA

David R. Williams

Center for Visual Science, University of Rochester, Rochester, NY, USA

The tuning properties of the ensemble of cone photoreceptors is due to the tuning properties of individual cones convolved with the disarray in pointing direction between the cones. We used direct imaging with the Rochester adaptive optics ophthalmoscope to directly image these properties in individual cones in living human eyes. We found that cone disarray is very small, accounting for less than 1% of the breadth of the tuning function of an ensemble of cones. The implication is that the optical fiber properties of an ensemble of cones mimic the tuning properties of a single cone.

Keywords: Stiles-Crawford effect, adaptive optics, photoreceptor disarray

Introduction

The Stiles-Crawford effect (Stiles & Crawford, 1933) describes the reduction in light sensitivity as its entry point moves to more peripheral locations in the pupil. It plays an important role in photopic vision because it rejects nonimaging light from the iris, sclera, and fundus and favors the light passing through the pupil center. This property is related to the waveguide properties of the cone photoreceptors (Enoch, 1963). However, because the Stiles-Crawford effect depends on aggregate signals from many cones, disarray in the pointing directions of individual cones is confounded with their angular tuning. Attempts to measure the angular tuning of single cones in excised primate retina are subject to artifact (Packer, Bensinger, & Williams, 1994). Based on the invariance of the angular tuning of a patch of cones with adaptation or bleaching by lights entering different parts of the pupil, MacLeod (MacLeod, 1974) and Burns et al. (Burns, Wu, He, & Elsner, 1996) inferred that the amount of disarray was small. Advances in retinal imaging with adaptive optics have allowed the first opportunity to measure directly these properties of individual cones in vivo. We show that there is very little disarray in the photoreceptors, and that this lack of disarray must be augmented in part by biomechanical factors in the retina. This result implies that objective measurements of the optical fiber properties of an ensemble of cones are essentially the same as for a single cone.

Methods

The measurement of the angular tuning properties of single cones was made possible by high-resolution imaging of individual cones with adaptive optics. This was accomplished in living human eyes using the Rochester adaptive optics ophthalmoscope. Two subjects were enrolled in the study. The research followed the tenets of the World Medical Association Declaration of Helsinki, informed consent was obtained from the subjects after we explained the nature and the possible complications of the study, and our experiments were approved by the University of Rochester Institutional Review Board.

Adaptive Optics Imaging

The adaptive optics technique is described in detail elsewhere (Liang, Williams, & Miller, 1997). In short, the optical aberrations of the eye that blur images of the retina are measured with a wavefront sensor and then compensated with a deformable mirror. Retinal images taken through the compensated optics are improved to the extent that the mosaic of cone photoreceptors can be resolved in a single image. This unprecedented image quality makes it possible to measure, for the first time, properties of individual cones in living human eyes (Roorda & Williams, 1999).

Angular Tuning

Although the ophthalmoscope detects reflected light, it was the acceptance angle of the cone that was actually measured in this experiment. This was done by measuring the amount of scattered light from each cone as we changed the angle of the illumination light. This measurement relies on the fact that the amount of light that gets scattered from a cone is directly related to the amount of light that gets coupled into the cone from the illumination light. This approach was adopted because it was necessary to image through as large a pupil as possible in order to resolve the cones. (Higher numerical aperture provides better image quality and is only accomplished in the human eye by imaging through a larger pupil.) Measuring the angular tuning of the reflected light would require moving a small exit pupil across the natural pupil,

DOI 10:1167/2.5.4 Received April 16, 2002; published September 17, 2002 ISSN 1534-7362

through which diffraction would limit the optical resolution. Also, the analysis would have been complicated because the reflected angular tuning from an ensemble of cones is further narrowed by the coherent interaction from the array of cones (Marcos & Burns, 1999, Marcos, Burns, & He, 1998).

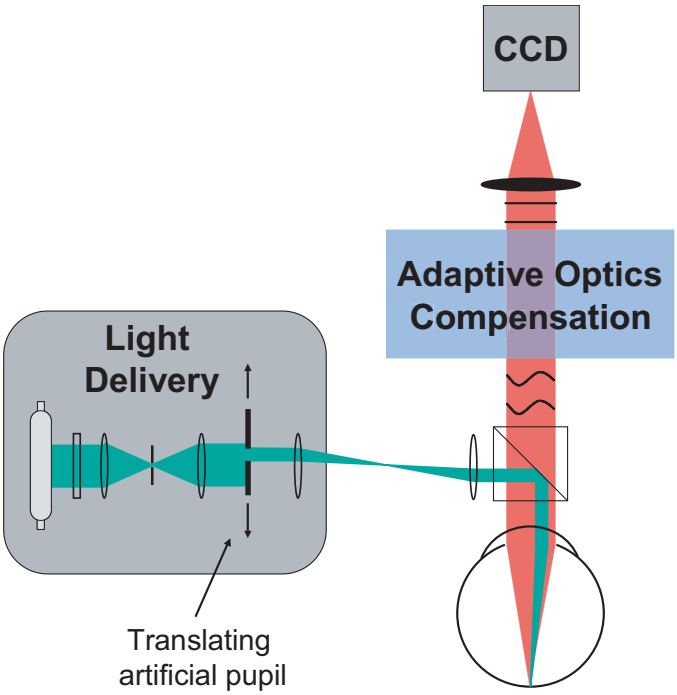

Figure 1. Adaptive optics ophthalmoscope for measuring angular tuning. Light from a krypton flashlamp is passed through a narrowband filter (550 nm, 70 nm bandwidth) and then through an artificial pupil. The pupil was translated in the beam to change the location of the entrance pupil, and, consequently, the illumination angle on the retina. Because the illumination angle was varied in this way, we had to correct the reflected intensity for nonuniformity in the illumination beam, which was measured after each experiment. Scattered light from the retina passed out of the eye, through the adaptive optics system and was imaged onto a scientific grade CCD camera.

The retina was illuminated through an artificial pupil, which was moved to different locations in the pupil to change the illumination angle. A schematic of the imaging system is shown in Figure 1. Reflectance images of the same patch of cone photoreceptors were taken with seven different entrance beam locations, one central and six locations in a surrounding ring. The location of the images for both subjects was 1 deg nasal from the fovea. Systematic changes in image quality that might have occurred during the course of the imaging session were avoided by randomizing the entrance beam locations, taking only two images at each location. Once seven pairs of images were collected from the seven locations, the wave aberration was recorrected and the random sequence was repeated until a total of 20 images were collected at each entrance beam location. The subject maintained a fully bleached state by looking into a bleaching lamp (550 nm, 70 nm bandwidth, 37 X 10^6 td-s) before each pair of images. The 10 best images at each location were selected, aligned with subpixel accuracy, and added together.

Results

Figure 2 shows a composite of images taken at seven different entrance beam locations. Because of cone directionality, the image taken with central illumination is the brightest and the images corresponding to peripheral illumination are dimmer. We identified the locations of a series of cones within a contiguous set from the central image. We then measured the average reflected intensity of each cone over a 3 X 3 pixel (0.42 X 0.42 arcmin) region around its center. Similarly, the intensity was measured at the same cone locations in the other six images, all of which were in register with the central image.

The following equation is the Gaussian angular tuning function representing the reflected intensity as a function of entrance beam location that was fit to the seven reflected intensities for each cone.

$$I_{pupilplane} = A \cdot \exp\left\{-\frac{(x-x_o)^2+(y-y_o)^2}{2\sigma^2}\right\} \quad (1)$$

where A is the peak reflectance, x_o and y_o define the location of peak reflectance in the entrance pupil plane (or the pointing direction), and σ is the spread of the angular tuning. We also calculated the 95% confidence intervals for each of the fitted parameters on each cone. This was important because in order to conclude confidently that there is disarray in a mosaic, the pointing direction of one cone must exceed the 95% range of the other. We chose not to include in our fit a constant term, which is often used to account for a nondirectional component in the reflection. The reason for omitting the constant term was because our 550-nm measurement wavelength was expected to give rise to only a small diffuse component in the reflection. The diffuse component was further reduced because we measured intensity from the centers of the cones, and not the spaces between them, where the nondirectional light would be expected to pass. Finally, our sampling geometry precluded fitting a constant nondirectional term with any degree of confidence.

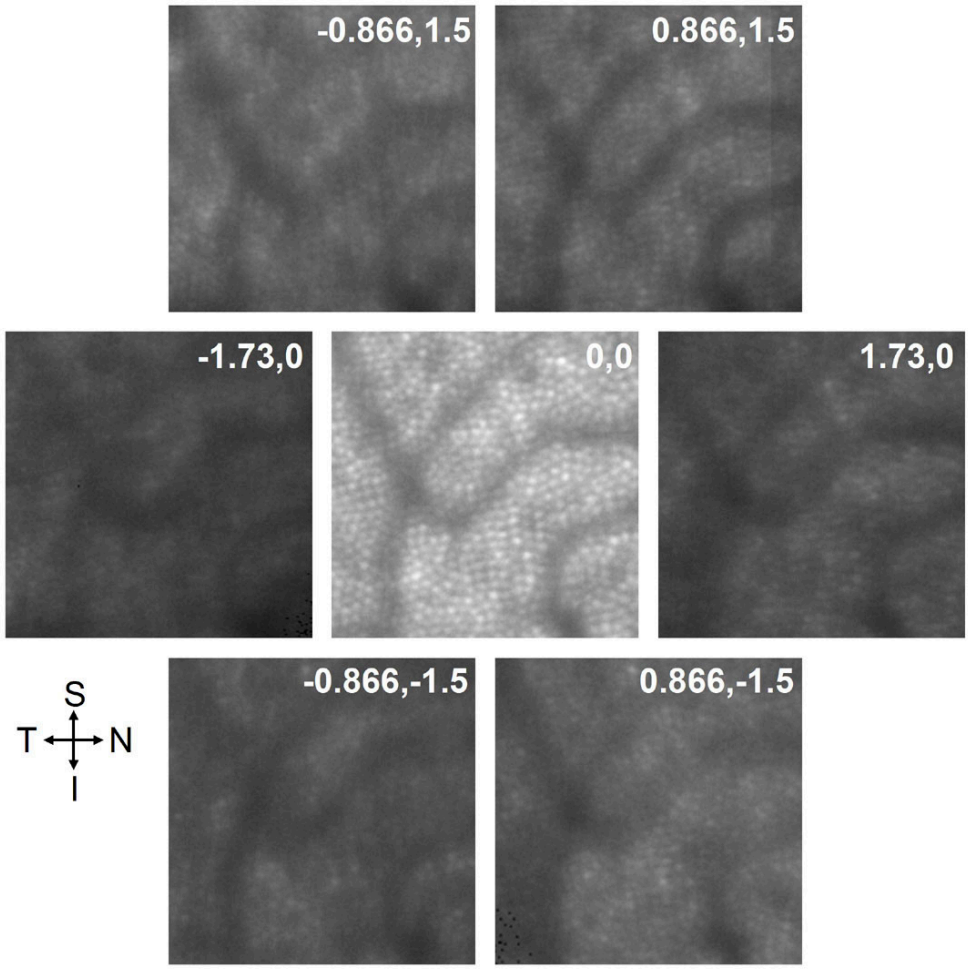

Figure 2. Composite of seven images of the same patch of retina taken with different entrance beam locations. Each image is a registered sum of 10 images. The number in the upper right corner of each image shows the position in mm of the entrance beam relative to the central illumination beam location. The central location was centered on our best estimation of the Stiles-Crawford peak. For J.P., the central location was 1.3 mm nasal and for G.Y. the location was at the geometrical center of the pupil. The symbols S, I, N, and T indicate the superior, inferior, nasal, and temporal directions in retinal space.

Angular tuning properties were measured over a contiguous array of cones in two subjects, J.P. (275 cones) and G.Y. (200 cones). The angular tuning function for each cone was fit using a least squares procedure. The results are illustrated in Figure 3 where the circles indicate the cone locations and the lines indicate the pointing direction and relative magnitude of departure of pointing direction from the average of the ensemble. These plots clearly show the presence of cone disarray. The plots also show that the disarray is systematic; there is local correlation in pointing direction among adjacent cones. We measured this local correlation by plotting the magnitude of the change in cone pointing direction as a function of cone separation (Figure 4). The data were fit with an exponential saturating function. The space constant, or the distance to where the function reached 64.3% of the saturation point, was similar for both subjects (3.1 arcmin for J.P. and 2.8 arcmin for G.Y.). The disarray is slightly greater in J.P. but the correlation distance is about the same. The most striking departures of pointing direction are seen in the vicinity of the blood vessels of subject J.P., who had particularly distinct blood vessels. This is because when the photoreceptor is illuminated through a light-absorbing blood vessel, there is less light reaching the photoreceptor. Consequently, less light reflects, causing the fit to show that it is pointing away from the vessel. Hence, we are not measuring the actual tuning function of the cone, but rather the effective tuning function. It should be noted that all in vivo measurements in the literature to date have been measuring the effective tuning function of the cones, although to different extents, depending on the specific absorption properties of the measurement wavelength that was used. An alternative explanation might be that cones actively point away from the blood vessels. However, this is unlikely given that cones do not reorient to compensate for the prismatic shift cause by the sloping foveal pit (Williams, 1980).

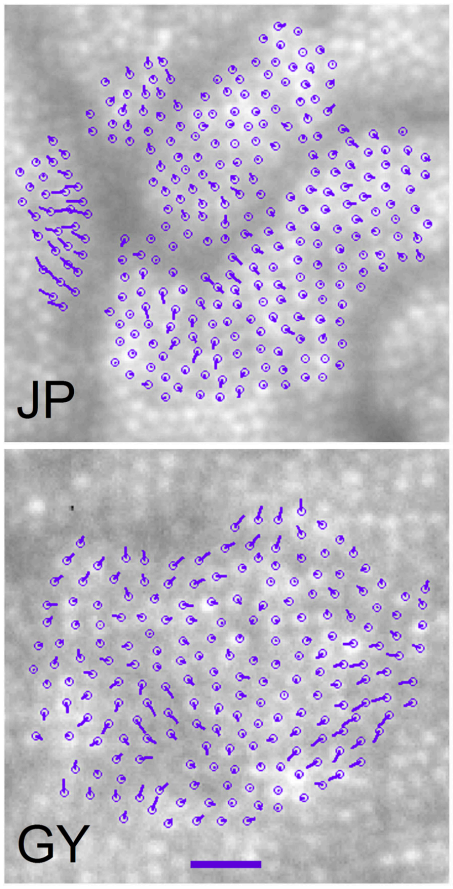

Figure 3. Cone directionality plots. The circles represent the cone locations and the lines represent the direction and magnitude of the departure of each cone's pointing direction in the pupil plane from the average of the ensemble. A displacement magnitude of 1 mm, which is about 2.5 deg of angular displacement, is indicated by the blue scale bar at the bottom of the figure.

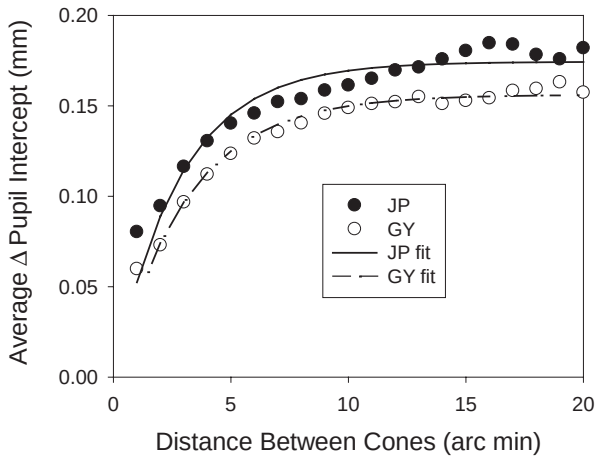

Figure 4. Correlation of directionality. The difference in pointing direction between cones increases, on average, with increasing cone separation. The closer cones are to each other, the more likely that they are pointing in the same direction. The lines show the best-fitting saturating exponential function.

Correction for Optical Blur

Although the adaptive optics technique improves resolution, the images are still not free from optical blur. The blur that remains is caused by diffraction, uncorrected aberrations, and a small amount of scattered light. Blurring causes the apparent angular tuning of a cone to depend on the angular tuning of its neighboring cones. This leads to an underestimate of the amount of disarray in the mosaic. In the limit, when the light from each cone in the patch is completely comingled in the image plane with light from its neighbors, then all cones will appear to point in the same direction. On the other hand, the presence of noise in the images will cause an overestimate in the amount of disarray.

Correcting for optical blur was possible because we had an estimate of the residual point spread function of the system (eye + AO ophthalmoscope) at image acquisition. This information was available because we used a Shack-Hartmann wavefront sensor to measure the aberration before and after adaptive optics correction in the AO ophthalmoscope.

The first step in correcting for optical blur was to generate an ideal cone mosaic using actual cone locations and diameters. Then we generated an ideal image series (like that shown in Figure 2) using various amounts of disarray and our best estimate of the individual cone angular tuning function, which was calculated as follows: The spread of the overall angular tuning function of the cones is the vector addition of the disarray and the angular tuning properties of the cones, as described in the following equation;

$$I_{pupilplane} = A \cdot \exp\left\{ - \frac{(x - x_o)^2 + (y - y_o)^2}{2 \times \left(\sigma^2_{disarray} + \sigma^2_{tuning}\right)} \right\} \qquad (2)$$

where A is the amplitude, x_o and y_o defines the average pointing direction of the ensemble of cones, and $\sigma_{disarray}$ and σ_{tuning} are the spreads for the disarray and tuning, respectively. This vector addition has the property so that when one term is much smaller than the other, it contributes negligibly to the overall tuning function. In our work, we found this to be the case; the measured disarray was about 5% of the tuning spread. We also determined that the blurring could cause a change in apparent disarray by a factor of 2 at most. Therefore, our estimation of the tuning function of the individual cones would have been essentially the same with or without optical blur, and so, for the simulation, its value was set to the initial estimated value. We added real estimates of the optical blur and noise to each of the images. (The noise was measured directly from the cones in the actual data set.) Then we computed the disarray of the simulated mosaic and compared it to the disarray that was input into the simulation. The process was repeated and we varied the initial disarray until the final

disarray matched what was measured in the experiment. The estimated disarray was the initial disarray that produced the closest postsimulation match to our measured result.

Correction for Finite Entrance Beam Aperture Diameter

Because the krypton flash lamp provided a limited amount of light, we were forced to illuminate the retina through a 2-mm and a 2.3-mm entrance pupil aperture for J.P. and G.Y., respectively. If we assumed the illumination was only through the center of the aperture, we would have overestimated the width of the tuning function. In the limit, with a large aperture, reflected intensity for all entrance pupil locations would be the same, the tuning function for each cone would appear flat and the pointing direction would be undefined. To correct for the finite aperture, we deconvolved the final tuning function of each cone with a circular aperture the size of the illumination aperture.

Comparison with Other Studies

A summary of the results before and after correction for blur, noise, and the finite entrance pupil diameter are listed in Table 1.

Our estimates of ρ are very close to those that have been collected in a similar manner (i.e., multiple-entry techniques described by Marcos & Burns, 1999). Incidentally, these ρ-values for angular tuning are about twice those of the Stiles-Crawford effect measured psychophysically (Applegate & Lakshminarayanan, 1993), but as yet there is no explanation for this difference. The current measurements are somewhat broader than those objective measurements (Burns, Wu, Delori, & Elsner, 1995; Gorrand & Delori, 1995; van Blokland, 1986) that are not immune to further narrowing due to coherent interaction of scattered light from the photoreceptor mosaic (Marcos & Burns, 1999).

Discussion

Though this method can easily measure the disarray among the cones, the main conclusion is that the disarray is, in fact, very small.

Figure 5 illustrates the lack of disarray when we project the axes of the disarrayed photoreceptors into the pupil plane of the eye. The average disarray has a full width at half maximum of 0.41 mm (from 0.17 sigma), which corresponds to an angle of 1 deg subtending only 13% of a 3-mm pupil diameter. The results are tabulated in Table 1. Corrections for blur, variations in illumination beam intensity, and effects of the finite aperture are included in the tabulated results.

Our results agree with Burns et al. (1996), Marcos and Burns (1999), and MacLeod (1974), all of whom concluded that there must be very little photoreceptor disarray. MacLeod calculated the disarray to be 0.32 mm (standard deviation of pupil intercept position), which is in reasonable agreement with our average finding of 0.17 mm. MacLeod's larger value may be due to the larger 2-deg test field size that he used versus our contiguous patch of cones of approximately 0.25-deg diameter. Our disarray is expected to be slightly narrower because of the correlation in pointing direction between neighboring cones. Furthermore, MacLeod measured the disarray 6 deg from the fovea compared to 1 deg for our measurement. Areal coverage by blood vessels anterior to the photoreceptors increases from zero at the foveal avascular zone to as high as 30% in the periphery (Snodderly, Weinhaus, & Choi, 1992), and a measurement of increased disarray in the periphery might be due to effective changes in the pointing direction of the cones caused by blood vessels.

Photoreceptor alignment is governed by a phototropic mechanism that actively aligns the cones to point toward the entrance pupil of the eye (Enoch & Lakshminarayanan, 1991). The best evidence for this is the active realignment of the Stiles-Crawford peak toward the pupil center in a patient following removal of a cataract that obscured all but the margin of the pupil on one side (Smallman, MacLeod, & Doyle, 2001).

Table 1. Cone Optical Waveguide Properties for Two Subjects

Subject	Average angular tuning		Average angular tuning after deconvolution with illumination aperture		Average pointing direction in pupil plane (mm)		Average photoreceptor disarray σ	
	ρ	σ	ρ	σ	X peak	Y peak	Measured	Estimated
J.P.	0.096	1.50 +/- 0.07	0.109	1.41	1.41	0.194	0.093	0.18
G.Y.	0.079	1.66 +/- 0.05	0.091	1.54	0.11	0.19	0.078	0.16

The angular tuning properties are expressed as both rho, ρ, and sigma, σ. The relationship between ρ and σ is: $\rho = 0.434/2\sigma^2$. All values are the mean (+/- 1 standard deviation) of 275 cones for J.P. and 200 cones for G.Y. The correction for the size of the finite aperture of the illumination beam narrowed the cone tuning function slightly and the disarray nearly doubled after correction for optical blur and noise.

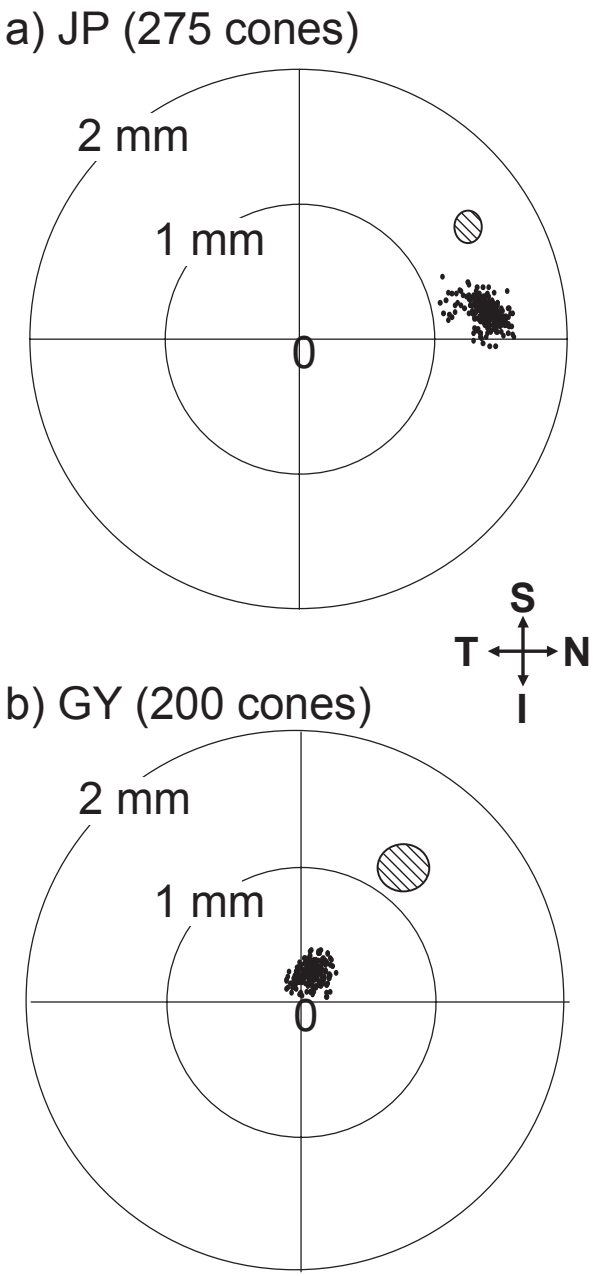

Figure 5. Pupil intercept plots. When the axes of the cones from Figure 3 are projected into the pupil plane, they are confined to a narrow distribution. Although the disarray is measurable and significant, the distribution is very narrow. The average 95% confidence limit in our ability to determine the cone pointing direction is shown as the shaded ellipse above the cone intercept distributions. The symbols S, I, N, and T indicate the superior, inferior, nasal, and temporal directions in pupil space.

The mechanism for realignment is unknown. Is the precision that we have observed in photoreceptor alignment the property of a phototropic mechanism in individual cones or groups of cones? A uniform pointing direction among the cones is desirable, but there is no clear benefit of the extent to which the cones are so uniformly aligned in the human eye. For example, the disarray we measured accounts for less than 1% of the breadth of the overall tuning function. A 4-fold increase in disarray for G.Y. would only broaden the overall tuning by 7.3%. Furthermore, any reduction in disarray will generate only tiny increases in detected image-forming light, or corresponding decreases in detected nonimaging light. These benefits are small, especially in light of the fact that J.P. detects about 25% fewer photons through a 4-mm pupil because his angular tuning peak is displaced 1.41-mm nasal. Displacements of this amount are common and average about 0.5 mm in the nasal direction (Dunnewold, 1964; Applegate & Lakshminarayanan, 1993). The idea that the alignment mechanism resides in each individual cone is not unreasonable given that motor movements of photoreceptors are reported in other vertebrate species (Burnside, 2001). A sophisticated feedback system is not a necessity for an individual cone mechanism to be effective because the fine alignment most likely is augmented by the physical properties of the ensemble of cones, which are long, thin, and close-packed into a nearly hexagonal matrix. Observations that implicate physical/biomechanical factors in controlling the directionality of cones in the retina have been those that disrupt ideal photoreceptor orientation. For example, shifts in pointing direction have been observed in large patches of photoreceptors near the optic disc of high myopes (Enoch, Choi, Kono, Lakshminarayanan, & Calvo, 2001) and in eyes with proliferative diabetic retinopathy (Bresnick, Smith, & Pokorny, 1981), both of which are thought to be caused by tractional forces in the retina. On a more local scale, cones demonstrate an inability to compensate for apparent peak displacements caused by prismatic effects along the slope of the foveal pit (Williams, 1980). This work identifies a case where the same biomechanical factors enhance the uniformity in pointing direction of the cones.

Conclusions

The lack of disarray in pointing direction in the cone photoreceptor array implies that any objective measurement of the tuning function of the cones in normal retina, whether it involves one, hundreds, or thousands of cones, will be almost identical to the effective tuning function of a single cone.

Acknowledgments

This work was supported in part by the National Science Foundation Science and Technology Center for Adaptive Optics, managed by the University of California at Santa Cruz under cooperative agreement No. AST-9876783 to A.R. and D.R.W., and by National Institute of Health Grants EY01319 and EY04367 to D.R.W. Commercial Relationships: None.

References

Applegate, R. A., & Lakshminarayanan, V. (1993). Parametric representation of Stiles-Crawford functions: Normal variation of peak location and directionality. *Journal of the Optical Society of America A*, *10*, 1611-1623. [PubMed]

Bresnick, G. H., Smith, V., & Pokorny, J., (1981). Visual function abnormalities in macular heterotopia caused by proliferative diabetic retinopathy. *American Journal of Ophthalmology*, *92*, 85-102. [PubMed]

Burns, S. A., Wu, S., Delori, F. C., & Elsner, A. E. (1995). Direct measurement of human-cone-photoreceptor alignment. *Journal of the Optical Society of America A*, *12*, 2329-2338. [PubMed]

Burns, S. A., Wu, S., He, J. C., & Elsner, A. E. (1996). Variations in photoreceptor directionality across the central retina. *Journal of the Optical Society of America A*, *14*, 2033-2040. [PubMed]

Burnside, B. (2001). Light and circadian regulation of retinomotor movement. In H. Kolb, H. Ripps, & S. Wu (Eds.), *Concepts and challenges in retinal biology: A tribute to John E. Dowling* (pp. 477-485). The Netherlands: Elsevier. [PubMed]

Dunnewold, C. J. W. (1964). On the Campbell and Stiles-Crawford effects and their clinical importance. Utrecht, The Netherlands: Rijksuniversiteit te Utrecht.

Enoch, J. M. (1963). Optical properties of the retinal receptors. *Journal of the Optical Society of America A*, *53*, 71-85.

Enoch, J. M., Choi, S. S., Kono, M., Lakshminarayanan, V., & Calvo, M. L. (2001). Receptor alignments and visual fields in high and low myopia. In M. Wall & R. P. Mills (Eds.), *Perimetry Update 2000/2001: Proceedings of the XIVth International Perimetric Society* (pp. 373-387). The Hague, The Netherlands: Kugler Publications.

Enoch, J. M., & Lakshminarayanan, V. (1991). Retinal fibre optics. In J. Cronly-Dillon (Ed.), *Vision and visual dysfunction* (Vol. 1, pp. 280-309). Boca Raton, FL: CRC Press.

Gorrand, J. -M., & Delori, F. C. (1995). A reflectometric technique for assessing photoreceptor alignment. *Vision Research*, *35*, 999-1010. [PubMed]

Liang, J., Williams, D. R., & Miller, D. (1997). Supernormal vision and high-resolution retinal imaging through adaptive optics. *Journal of the Optical Society of America A*, *14*, 2884-2892. [PubMed]

MacLeod, D. I. A. (1974). Directionally selective light adaptation: A visual consequence of receptor disarray? *Vision Research*, *14*, 369-378. [PubMed]

Marcos, S., & Burns, S. A. (1999). Cone spacing and waveguide properties from cone directionality measurements. *Journal of the Optical Society of America A*, *16*, 995-1004. [PubMed]

Marcos, S., Burns, S. A., & He, J. C. (1998). Model for cone directionality reflectometric measurements based on scattering. *Journal of the Optical Society of America A*, *15*, 2012-2022. [PubMed]

Packer, O., Bensinger, D. G., & Williams, D. R. (1994). In vitro angular tuning of single primate rods and cones and the Stiles-Crawford effect [Abstract]. *Investigative Ophthalmology and Visual Science*, *35*, 1572.

Roorda, A., & Williams, D. R. (1999). The arrangement of the three cone classes in the living human eye. *Nature*, *397*, 520-522. [PubMed]

Smallman, H. S., MacLeod, D. I. A ., & Doyle, P. (2001). Realignment of cones after cataract removal. *Nature*, *412*, 604-605. [PubMed]

Snodderly, D. M., Weinhaus, R. S., & Choi, J. C. (1992). Neural-vascular relationships in central retina of Macaque monkeys (Macaca fascicularis). *Journal of Neuroscience*, *12*, 1169-1193. [PubMed]

Stiles, W. S., & Crawford, B. H. (1933). The luminous efficiency of rays entering the eye pupil at different points. *Proceedings of the Royal Society of London. Series B: Biological Sciences*, *112*, 428-450.

van Blokland, G. J. (1986). Directionality and alignment of the foveal receptors, assessed with light scattered from the human fundus in vivo. *Vision Research*, *26*, 495-500. [PubMed]

Williams, D. R. (1980). Visual consequences of the foveal pit. *Investigative Ophthalmology and Visual Science*, *19*, 653-667. [PubMed]